M. TREPCZYŃSKA-ŁENT[1*]

CHARACTERISTICS OF THE GROWTH OF THE DIRECTIONALLY SOLIDIFIED Fe-4.25% C EUTECTIC ALLOY

The current work is dedicated to the mathematical description of a protrusion of the leading phase (cementite) over the wetting phase (austenite) observed during the author's experiments in previous articles. A cementite protrusion is confirmed in the directionally solidified Fe-4.25% C eutectic alloy. The protrusion is defined due to the mass balance fulfilment. A coordinate system is attached to the solid/liquid interface, which is moving with the constant growth rate v.

Keywords: Fe-C eutectic alloy, directional solidification, protrusion of leading phase

Symbols used in the text

C – solute concentration in the liquid,

C_E – solute concentration at the eutectic point,

$C_0^{Fe_3C}$ – concentration of the cementite at the solubility limit point at temperature T_E,

$C_0^{Fe(\gamma)}$ – concentration of the austenite at the solubility limit point at temperature T_E,

$C_S^{Fe_3C}$ – equilibrium solute concentration in the Fe_3C – phase lamella,

$C_S^{Fe(\gamma)}$ – equilibrium solute concentration in the $Fe(\gamma)$ – phase lamella,

D – diffusion coefficient in the liquid,

d_{Fe_3C} – protrusion of the cementite phase above the wetting phase,

$d_{Fe(\gamma)}$ – delay of the wetting austenite phase,

$Fe(\gamma)$ – wetting eutectic austenite phase,

Fe_3C – leading eutectic cementite phase,

$f(x)$ – function used to describe the interface shape,

$f_1(x)$ – function used in formulation of s/l interface for the Fe_3C phase,

$f_2(x)$ – function used in formulation of s/l interface for the $Fe(\gamma)$ phase,

$f_{Fe(\gamma)}$ – function used in formulation of boundary condition for the $Fe(\gamma)$ phase,

f_{Fe_3C} – function used in formulation of boundary condition for the Fe_3C phase,

m – slope of liquidus line,

m_{Fe_3C} – slope of liquidus line at the Fe_3C phase,

$m_{Fe(\gamma)}$ – slope of liquidus line at the $Fe(\gamma)$ phase,

S_{Fe_3C} – half the width of the cementite – phase lamellae,

$S_{Fe(\gamma)}$ – half the width of the austenite – phase lamellae,

T – temperature,

T_E – equilibrium eutectic temperature,

$tg\,\theta_{Fe(\gamma)}$ – tangent of the contact angle of $Fe(\gamma)$ phase,

$tg\,\theta_{Fe_3C}$ – tangent of the contact angle of Fe_3C phase,

v – growth rate,

ΔC_∞ – eutectic difference of the C_E solute concentration and its concentration in the initial alloy,

δC – concentration field in the liquid ahead the s/l interface,

Φ_{Fe_3C} – volume fraction of the Fe_3C phase,

$\Phi_{Fe(\gamma)}$ – volume fraction of the $Fe(\gamma)$ phase,

Γ_{Fe_3C} – capillary length of the Fe_3C phase,

$\Gamma_{Fe(\gamma)}$ – capillary length of the $Fe(\gamma)$ phase,

λ – interphase (interlamellar) spacing for regular structure,

Π', P – alloy material constant,

$\overline{\Delta T}$ – general undercooling,

ΔT_c – diffusion undercooling of the s/l interface,

ΔT_r – curvature undercooling of the s/l interface,

ΔT_{Fe_3C} – undercooling of the s/l interface of the Fe_3C phase,

$\Delta T_{Fe(\gamma)}$ – undercooling of the s/l interface of the $Fe(\gamma)$ phase,

θ_{Fe_3C} – contact angle of Fe_3C phase,

$\theta_{Fe(\gamma)}$ – contact angle of $Fe(\gamma)$ phase.

[1] UTP UNIVERSITY OF SCIENCE AND TECHNOLOGY, MECHANICAL ENGINEERING FACULTY, BYDGOSZCZ, POLAND

* Corresponding author: malgorzata.trepczynska-lent@utp.edu.pl

1. Introduction

Eutectics are an archetype of composite materials with a fine microstructure in the µm scale, the properties of which are controlled by solidification conditions. These composites *in situ* have been studied for decades due to their excellent mechanical properties. In the past, researchers' attention has focused mainly on metallic eutectics, and most of the progress in understanding eutectic growth and microstructure has been achieved in these materials, [1-5].

The vast majority of technical eutectic alloys consist of two phases. Solidification of double or pseudo-double eutectics may lead to the formation of regular lamellar or fibrous structures, [1,6]. The eutectic growth described by the coupled growth of the solid phase from liquid is an important model for crystal growth, [1,6]. Understanding eutectic growth dynamics is a key aspect of eutectic system research.

Eutectic growth is a typical diffusion controlled process. Therefore, the solution to this problem depends on how to analyse the diffusion field on the solid/liquid interface. The purpose of these analyses is to determine the relationship between under-cooling ΔT, growth rate v and interphase spacing λ.

2. Research material and experimental procedure

The sample of Fe-4.25 wt.% C eutectic alloy, made of high purity Armco and graphite electrodes, was prepared in a corundum crucible under an argon gas shield in a Balzers type heater. After removing the dross and thermal stabilization the molten alloy was cast into a rod of 12 mm diameter. The sample was machined to approximately 5 mm and:

a) placed in an alunde tube (6 mm inner diameter) in the vacuum Bridgman-type furnace, under an argon atmosphere,
b) heated to a temperature of 1450°C,
c) after stabilizing the thermal conditions, lowered from the heating part, at a given rate, to the cooling part of the furnace,
d) grown up to 30 mm in length at a constant temperature gradient $G = 33.5$ K/mm by pulling it down at a constant pulling rate $v = 125$ µm/s,
e) rapidly quenched by being pulled down into the Ga-In-Sn liquid metal.

The research of directional solidification was performed at the Faculty of Foundry Engineering, Department of Engineering of Cast Alloys and Composites at the AGH University of Science and Technology in Krakow. The procedure of the experiment is defined in more detail in [7-9]. The directional solidification studies of this alloy are described in [10,11].

Chemical composition of Fe-4.25% C alloy is shown in Table 1.

Considering that overall the dimensions of the leading phase are smaller than the dimensions of wetting phase, it should be stated that the leading phase of the examined alloy is the cementite phase (Fig. 1) [12].

The Figure 1 shows scheme of solid/liquid interface of quasi-regular Fe-4.25% C eutectic alloy. The width of the cementite phase lamellae – $2S_{Fe_3C}$ is smaller than the width of austenite phase (pearlite) – $2S_{Fe(\gamma)}$ width ($S_{Fe(\gamma)} > S_{Fe_3C}$). Therefore, in the studied eutectic alloy, cementite is the leading phase as indicated by convexity of d_{Fe_3C} cementite phase [12]. The concave of austenite phase – $d_{Fe(\gamma)}$ and convexity of d_{Fe_3C} cementite phase are shown.
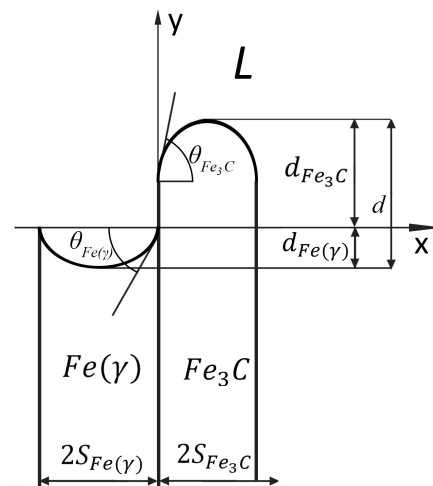

Fig. 1. Coordinate system and contact angles at the triple point of the convex-concave solid/liquid interface and definitions of the width of both eutectic phases: d_{Fe_3C} – convexity of cementite phase, $d_{Fe(\gamma)}$ – concave of austenite phase, d – total protrusion of Fe_3C phase

3. Analysis of eutectic growth according to the Guzik model

The Guzik model [13] comes from the mass diffusion equation:

$$\frac{\partial^2 C}{\partial x^2} + \frac{\partial^2 C}{\partial y^2} + \frac{v}{D}\frac{\partial C}{\partial y} = 0 \tag{1}$$

TABLE 1

Chemical composition of Fe-4.25% C alloy [wt. %]

C	Si	Mn	P	S	Cr	Ni	Mo	Al	Cu
4.25	0.057	0.64	0.0079	0.021	0.033	0.0093	<0.0020	0.011	0.032
Co	Ti	Ni	Nb	V	W	Pb	Mg	B	Sn
0.0024	<0.0010	0.0093	<0.0040	0.0022	<0.010	<0.0030	<0.0010	0.0009	0.0061
Zn	As	Bi	Ca	Ce	Zr	La	Fe		
<0.0020	0.0069	<0.0020	0.0005	<0.0030	0.0043	0.0013	94.9		

which under specified boundary conditions and mass balance conditions at the s/l interface allows to determine the concentration field in the liquid phase ahead of the s/l interface:

$$
C_{(x,y)} = C_E + \Delta C_\infty + B_0 \exp\left(-\frac{v\,y}{D}\right) +
$$

$$
+ \sum_{n=1}^{\infty} B_n \, \cos\left(\frac{n\,2\pi\left(x - S_{\mathrm{Fe_3C}}\right)}{\lambda}\right) \exp\left(-\frac{n\,2\pi\,y}{\lambda}\right) \quad (2)
$$

where:

$$
B_0 = C_0^{\mathrm{Fe_3C}} \Phi_{\mathrm{Fe_3C}} - C_0^{\mathrm{Fe}(\gamma)} \Phi_{\mathrm{Fe}(\gamma)} \quad (3)
$$

$$
B_n = \frac{\lambda}{(n\pi)^2} \frac{v}{D} C_0 \, \sin\left(n\pi \, \Phi_{\mathrm{Fe_3C}}\right) \quad (4)
$$

$$
C_0 = C_0^{\mathrm{Fe_3C}} + C_0^{\mathrm{Fe}(\gamma)} \quad (5)
$$

Guzik [13], for growth analysis, attached x-y coordinate system at the triple point of the solid/liquid interphase. It moved in the direction of the y axis.

A constant eutectic growth rate v and a constant temperature gradient G in the liquid at the s/l interface were assumed. To describe the s/l interface shape of cementite and austenite phases, an even square function was used, which was symmetrical in relation to the y axis:

$$
f(x) = ax^2 + bx + c \quad (6)
$$

This function was chosen, due to the analysis of Magnin and Kurz [14] study.

Boundary conditions for the Fe$_3$C – faceted phase were determined:

$$
f_1\left(-S_{\mathrm{Fe_3C}}\right) = d_{\mathrm{Fe_3C}} \quad (7)
$$

$$
f_1(0) = 0 \quad (8)
$$

$$
\left(\frac{df_1}{dx}\right)_0 = \mathrm{tg}\left(180° - \theta_{\mathrm{Fe_3C}}\right) = -\mathrm{tg}\,\theta_{\mathrm{Fe_3C}} \quad (9)
$$

$$
\left(\frac{df_1}{dx}\right)_{-S_{\mathrm{Fe_3C}}} = 0 \quad (10)
$$

For the non-faceted phase, the following boundary conditions are given:

$$
f_2\left(S_{\mathrm{Fe}(\gamma)}\right) = -d_{\mathrm{Fe}(\gamma)} \quad (11)
$$

$$
f_2(0) = 0 \quad (12)
$$

$$
\left(\frac{df_2}{dx}\right)_0 = \mathrm{tg}\,\theta_{\mathrm{Fe}(\gamma)} \quad (13)
$$

$$
\left(\frac{df_2}{dx}\right)_{S_{\mathrm{Fe}(\gamma)}} = 0 \quad (14)
$$

Conditions given by Eq. (7) and Eq. (11) are related to the value of protrusion of the carbide faceted phase $d_{\mathrm{Fe_3C}}$ and the delay of the non-faceted phase $d_{\mathrm{Fe}(\gamma)}$. Further conditions Eq. (8-10) and Eq. (12-14) are a consequence of the shape of the s/l interface adopted. The sought functions $f_1(x)$ and $f_2(x)$ for the adopted boundary conditions can be written:

– for the Fe$_3$C faceted phase:

$$
f_1(x) =
$$
$$
= \left(\frac{\mathrm{tg}\,\theta_{\mathrm{Fe}(\gamma)}}{\lambda \, \Phi_{\mathrm{Fe_3C}}} - \frac{8\,d_{\mathrm{Fe_3C}}}{\lambda^2 \, \Phi_{\mathrm{Fe_3C}}^2}\right)\left(x + S_{\mathrm{Fe_3C}}\right)^2 + d_{\mathrm{Fe_3C}} \quad (15)
$$

– for the Fe(γ) nonfaceted phase:

$$
f_2(x) =
$$
$$
= \left(\frac{8\,d_{\mathrm{Fe}(\gamma)}}{\Phi_{\mathrm{Fe}(\gamma)}^2 \, \lambda^2} - \frac{3\,\mathrm{tg}\,\theta_{\mathrm{Fe}(\gamma)}}{\lambda \, \Phi_{\mathrm{Fe}(\gamma)}}\right)\left(x - S_{\mathrm{Fe}(\gamma)}\right)^2 - d_{\mathrm{Fe}(\gamma)} \quad (16)
$$

The following nonisothermal coupling condition is given:

$$
\frac{1}{S_{\mathrm{Fe_3C}}} \int_{-S_{\mathrm{Fe_3C}}}^{0} \left[\Delta T_c(x) + \Delta T_r(x) + G f_1(x)\right] dx =
$$
$$
= \frac{1}{S_{\mathrm{Fe}(\gamma)}} \int_{0}^{S_{\mathrm{Fe}(\gamma)}} \left[\Delta T_c(x) + \Delta T_r(x) + G f_2(x)\right] dx = \overline{\Delta T} \quad (17)
$$

The components of general undercooling $\overline{\Delta T}$, ΔT_c components associated with the diffusion process, and the ΔT_r solidification front curvature were adopted according to the Jackson-Hunt theory, [15,16].

Further components of the equation (17) are as follows:

$$
\frac{1}{S_{\mathrm{Fe}(\gamma)}} \int_{0}^{S_{\mathrm{Fe}(\gamma)}} \Delta T_c(x)\, dx =
$$
$$
= \frac{1}{S_{\mathrm{Fe}(\gamma)}} \int_{0}^{S_{\mathrm{Fe}(\gamma)}} m_{\mathrm{Fe}(\gamma)}\left[C_E - C_{(x,0)}\right] =
$$
$$
= -m_{\mathrm{Fe}(\gamma)}\left(\Delta C_\infty + B_0 + \frac{\lambda v C_0 P_{\mathrm{Fe}(\gamma)}}{\Phi_{\mathrm{Fe}(\gamma)} D}\right) \quad (18)
$$

$$
\frac{1}{S_{\mathrm{Fe_3C}}} \int_{-S_{\mathrm{Fe_3C}}}^{0} \Delta T_c(x)\, dx =
$$
$$
= -m_{\mathrm{Fe_3C}}\left(\Delta C_\infty + B_0 + \frac{\lambda v C_0 P_{\mathrm{Fe_3C}}}{\Phi_{\mathrm{Fe_3C}} D}\right) \quad (19)
$$

$$
\frac{1}{S_{\mathrm{Fe}(\gamma)}} \int_{0}^{S_{\mathrm{Fe}(\gamma)}} \Delta T_r(x)\, dx = \frac{2\,\Gamma_{\mathrm{Fe}(\gamma)} \sin\theta_{Fe(\gamma)}}{\Phi_{\mathrm{Fe}(\gamma)}\,\lambda} \quad (20)
$$

$$
\frac{1}{S_{\mathrm{Fe_3C}}} \int_{-S_{\mathrm{Fe_3C}}}^{0} \Delta T_r(x)\, dx = \frac{2\,\Gamma_{\mathrm{Fe_3C}} \sin\theta_{\mathrm{Fe_3C}}}{\Phi_{\mathrm{Fe_3C}}\,\lambda} \quad (21)
$$

$$\frac{1}{S_{Fe(\gamma)}}\int_{0}^{S_{Fe(\gamma)}} Gf_2(x)\,dx =$$

$$= -\frac{G\,\mathrm{tg}\,\theta_{Fe(\gamma)}\,\lambda\,\Phi_{Fe(\gamma)}}{1,5} - \frac{8G\,d_{Fe(\gamma)}}{15} \qquad (22)$$

$$\frac{1}{S_{Fe_3C}}\int_{-S_{Fe_3C}}^{0} Gf_1(x)\,dx =$$

$$= \frac{G\,\mathrm{tg}\,\theta_{Fe_3C}\,\lambda\,\Phi_{Fe_3C}}{1,5} + \frac{8G\,d_{Fe_3C}}{15} \qquad (23)$$

Substituting equations (18-23) into equation (17):

$$\overline{\Delta T_{Fe(\gamma)}} = -m_{Fe(\gamma)}\left(\Delta C_\infty + B_0 + \frac{\lambda v C_0 P_{Fe(\gamma)}}{\Phi_{Fe(\gamma)}D}\right) +$$

$$+ \frac{2\Gamma_{Fe(\gamma)}\sin\theta_{Fe(\gamma)}}{\Phi_{Fe(\gamma)}\lambda} + \left(-\frac{G\,\mathrm{tg}\,\theta_{Fe(\gamma)}\lambda\,\Phi_{Fe(\gamma)}}{1,5} - \frac{8G\,d_{Fe(\gamma)}}{15}\right) \qquad (24)$$

$$\overline{\Delta T_{Fe_3C}} = -m_{Fe_3C}\left(\Delta C_\infty + B_0 + \frac{\lambda v C_0 P_{Fe_3C}}{\Phi_{Fe_3C}D}\right) +$$

$$+ \frac{2\Gamma_{Fe_3C}\sin\theta_{Fe_3C}}{\Phi_{Fe_3C}\lambda} + \left(\frac{G\,\mathrm{tg}\,\theta_{Fe_3C}\lambda\,\Phi_{Fe_3C}}{1,5} + \frac{8G\,d_{Fe_3C}}{15}\right) \qquad (25)$$

The following formulas can be introduced:
the protrusion of the Fe$_3$C faceted phase relative to the Fe(γ) phase:

$$d_{Fe_3C} = \frac{15\,\Phi_{Fe_3C}^2}{7G\lambda^2\Phi_{Fe_3C}^2 + 240\Gamma_{Fe_3C}} \times$$

$$\times \left[\begin{array}{l} \dfrac{m_{Fe_3C}C_0 v}{D}\left(\Pi'_{Fe_3C} - \dfrac{P}{\Phi_{Fe_3C}}\right) + \\[2ex] + \dfrac{G\Phi_{Fe_3C}\,\mathrm{tg}\,\theta_{Fe_3C}}{30}\lambda^3 + \\[2ex] + \dfrac{2\Gamma_{Fe_3C}\lambda}{\Phi_{Fe_3C}}\left(\mathrm{tg}\,\theta_{Fe_3C} + \sin\theta_{Fe_3C}\right)\end{array}\right] \qquad (26)$$

the delay of the nonfaceted phase Fe(γ):

$$d_{Fe(\gamma)} = \frac{15\,\Phi_{Fe(\gamma)}^2}{7G\lambda^2\Phi_{Fe(\gamma)}^2 + 240\Gamma_{Fe(\gamma)}} \times$$

$$\times \left[\begin{array}{l} \dfrac{|m_{Fe(\gamma)}|C_0 v}{D}\left(\Pi'_{Fe(\gamma)} - \dfrac{P}{\Phi_{Fe(\gamma)}}\right) + \\[2ex] + \dfrac{G\Phi_{Fe(\gamma)}\,\mathrm{tg}\,\theta_{Fe(\gamma)}}{1,5}\lambda^3 + \\[2ex] + \dfrac{2\Gamma_{Fe(\gamma)}\lambda}{\Phi_{Fe(\gamma)}}\left(3\mathrm{tg}\,\theta_{Fe(\gamma)} - \sin\theta_{Fe(\gamma)}\right)\end{array}\right] \qquad (27)$$

For the studied directionally solidified Fe-4.25%C eutectic alloy, the relationship between interphase (interlamellar) spacing λ and growth rate v, is given by the formula from [12]:

$$\lambda = -0.0405 v^{-0.5} + 11.499 \qquad (28)$$

Substituting equation (28) into equation (26):

$$d_{Fe_3C} =$$

$$= \frac{15\,\Phi_{Fe_3C}^2}{7G\left(-0.0405 v^{-0,5}+11.499\right)^2\Phi_{Fe_3C}^2 + 240\Gamma_{Fe_3C}} \times$$

$$\times \left[\begin{array}{l} \dfrac{m_{Fe_3C}C_0 v}{D}\left(\Pi'_{Fe_3C} - \dfrac{P}{\Phi_{Fe_3C}}\right) + \\[2ex] + \dfrac{G\Phi_{Fe_3C}\,\mathrm{tg}\,\theta_{Fe_3C}}{30}\left(-0.0405 v^{-0.5}+11.499\right)^3 + \\[2ex] + \dfrac{2\Gamma_{Fe_3C}\left(-0.0405 v^{-0.5}+11.499\right)}{\Phi_{Fe_3C}} \times \\[2ex] \times\left(\mathrm{tg}\,\theta_{Fe_3C} + \sin\theta_{Fe_3C}\right)\end{array}\right] \qquad (29)$$

Equations (26) and (27) define the protrusion of the leading phase (cementite) and the delay of the wetting phase (austenite), respectively. Eq. (29) shows the relationship of protrusion of the leading cementite phase between growth rate for studied directionally solidified Fe-4.25%C eutectic alloy.

4. Analysis of eutectic growth according to the Wołczyński model

Observation of the concave-convex front of solidification and its scheme (Fig. 2) shows that the lamellae of both phases are almost equal in width, or that the width of the cementite phase is slightly smaller. Therefore, assumptions found in the literature, [17,18] can be used to analyse the growth of the researched cast iron.

Considering the facts that the local mass balance is met for the condition $z = 0$ in the case of a wider Fe(γ) phase lamellar, and assuming that $z = d$ for the narrower Fe$_3$C phase lamellar, the boundary mass balance is also considered at the same location.

The existence of protrusion d has been disclosed and described theoretically, [19-21]. It has been experimentally confirmed that usually the finer (smaller dimensionally) phase is the leading phase, [20,21]. This corresponds to the analysis of the local mass balance shown in the work, [17] by Equations (31), (32), (33) and Eq. (33*). Accordingly, protrusion is only observed for the phase with smaller (narrower) lamellar.

In order to determine the value of the advance parameter for the examined eutectics Fe(γ) – 4.25% C, the Wołczyński equation from [17] was used. It allows to define the phase protrusion d for the leading phase for own Bridgman experiment.

Figure 2 shows the protrusion scheme for the solid/liquid interface described by the experiment performed in [7,8]. For this
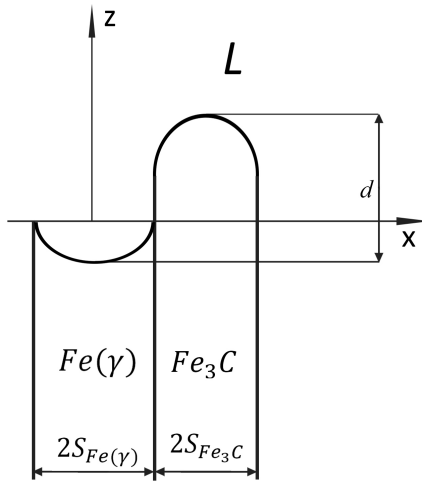
Fig. 2. Coordinate system attached at the s/l interface moving with thzgrowth rate v of the quasi-regular Fe-4.25% C eutectic alloy for the Wołczyński model

condition, there is a condition for the nonisothermal s/l interface of regular eutectics:

$$\Delta T_{\text{Fe}(\gamma)} \neq \Delta T_{\text{Fe}_3\text{C}} \tag{30}$$

$$C_0^{\text{Fe}(\gamma)}\left(S_{\text{Fe}_3\text{C}},0\right) = C_S^{\text{Fe}(\gamma)}\left(S_{\text{Fe}(\gamma)},0\right) - C_E < 0 \tag{31}$$

$$C_0^{\text{Fe}_3\text{C}}\left(S_{\text{Fe}_3\text{C}},0\right) = C_S^{\text{Fe}_3\text{C}}\left(S_{\text{Fe}_3\text{C}},0\right) - C_E > 0 \tag{32}$$

For the stationary eutectic growth, the diffusion equation is, [16]:

$$\frac{\partial^2 \delta C}{\partial x^2} + \frac{\partial^2 \delta C}{\partial z^2} + \frac{v}{D}\frac{\partial \delta C}{\partial z} = 0 \tag{33}$$

The solution to Eq. (33) can be given as:

$$\delta C(x,z) = X(x)Z(z) \tag{34}$$

with the coordinate system attached to the s/l interface just at the middle of the Fe(γ) – phase lamella (Fig. 2).

New boundary condition has been inserted in the current description:

$$\delta C\left(S_{\text{Fe}(\gamma)},z\right) = C\left(S_{\text{Fe}(\gamma)},z\right) - C_E = 0 \tag{35}$$

The Jackson and Hunt theory [15] does not consider Eq. (35). Nevertheless, the assumption given by Eq. (35) does not allow a discontinuity of solute undercooling (constitutional undercooling) to appear. This results in micro-field of the temperature at the s/l interface. Therefore,

$$Z(z) = \exp\left[\left(-\frac{v}{2D} - \sqrt{\frac{v^2}{4D^2} + \omega^2}\right)z\right] \tag{36}$$

$$X(x) = A\cos(\omega x) + B\sin(\omega x) \tag{37}$$

The other boundary conditions are like the ones used in the Jackson and Hunt theory:

$$\frac{\partial C}{\partial x} = 0 \text{ for } x = 0, \text{ and } x = S_{\text{Fe}(\gamma)} + S_{\text{Fe}_3\text{C}} \tag{38}$$

$$\frac{\partial C}{\partial z} = \mp\frac{v C_0^S}{D} \text{ for } S = \text{Fe}(\gamma), \text{Fe}_3\text{C},$$
$$z = 0, \ 0 \leq x < S_{\text{Fe}(\gamma)}, \ S_{\text{Fe}(\gamma)} < x \leq S_{\text{Fe}(\gamma)} + S_{\text{Fe}_3\text{C}} \tag{39}$$

After some transformations, and with the plane s/l interface applied, the description of the solute micro-field ahead of the s/l interface is:

A) For the Fe(γ) – eutectic phase, that is for $x \in [0, S_{\text{Fe}(\gamma)}]$, $z \geq 0$.

The value of the parameters B and ω is a result of the following (modified) condition:

$$\left.\frac{\partial \delta C(x,z)}{\partial x}\right|_{x=0} = 0 \tag{40}$$

Therefore, the formula: $-\omega A\sin(\omega 0) + \omega B\cos(\omega 0) = 0$ it results in $B = 0$.

Furthermore:

$$\omega = \omega_{2n-1} = \frac{(2n-1)\pi}{2S_{\text{Fe}(\gamma)}}, \ n = 1,2,3,\dots \tag{41}$$

Combining Eq. (34), Eq. (37) with Eq. (35) and Eq. (40) the solution to Eq. (33) is:

$$\delta C(x,z) = \sum_{n=1}^{\infty} A_{2n-1}\cos\left(\frac{(2n-1)\pi x}{2S_{\text{Fe}(\gamma)}}\right) \times$$
$$\times \exp\left[\left(-\frac{v}{2D} - \sqrt{\frac{v^2}{4D^2} + \left(\frac{(2n-1)\pi}{2S_{\text{Fe}(\gamma)}}\right)^2}\right)z\right] \tag{42}$$

where, A_{2n-1}, is constant.

To define the A_{2n-1} parameter, the following conditions are required:

$$\left.\frac{\partial \delta C(x,z)}{\partial z}\right|_{z=0} = f_{\text{Fe}(\gamma)}(x);$$
$$f_{\text{Fe}(\gamma)}(x) < 0, x \in \left[0, S_{\text{Fe}(\gamma)}\right] \ f_{\text{Fe}(\gamma)}(x) \neq 0 \tag{43}$$

thus:

$$\left.\frac{\partial \delta C(x,z)}{\partial z}\right|_{z=0} =$$
$$= \sum_{n=1}^{\infty} A_{2n-1}\left(\begin{array}{c} -\frac{v}{2D} - \sqrt{\frac{v^2}{4D^2} + \left(\frac{(2n-1)\pi}{2S_{\text{Fe}(\gamma)}}\right)^2} \times \\ \times \cos\left(\frac{(2n-1)\pi x}{2S_{\text{Fe}(\gamma)}}\right) \end{array}\right) \tag{44}$$

1184

The following properties of introduced function $f(x)$ are worth noting:

$$f(x) - 2S_{Fe(\gamma)} \leq x \leq 2S_{Fe(\gamma)},$$
$$f(-x) = f(x), \quad f(x + 2S_{Fe(\gamma)}) = -f(x) \tag{45}$$

$$f(x) \approx \frac{a_0}{2} + \sum_{n=1}^{\infty} a_n \cos\left(\frac{n\pi x}{2S_{Fe(\gamma)}}\right) \tag{46}$$

$$a_n = \frac{1}{S_{Fe(\gamma)}} \int_0^{2S_{Fe(\gamma)}} f(x) \cos\left(\frac{n\pi x}{2S_{Fe(\gamma)}}\right) dx \tag{47}$$

Assuming:

$$f(x + 2S_{Fe(\gamma)}) = -f(x) \tag{48}$$

it results in: $a_{2k} = 0$, $k = 0, 1, 2, ...$ for $n = 2k$

$$a_{2k-1} = \frac{2}{S_{Fe(\gamma)}} \int_0^{S_{Fe(\gamma)}} f(x) \cos\left(\frac{(2k-1)\pi x}{2S_{Fe(\gamma)}}\right) dx \tag{49}$$

$k = 1, 2...$ for $n = 2k-1$, $k = 1, 2, ...$

The Fourier's series for $f(x)$ can be presented as:

$$f(x) \approx \sum_{k=1}^{\infty} a_{2k-1} \cos\left(\frac{(2k-1)\pi x}{2S_{Fe(\gamma)}}\right) \tag{50}$$

In conclusion, the parameter A_{2n-1} is defined:

$$A_{2n-1} = \left(-\frac{v}{2D} - \sqrt{\frac{v^2}{4D^2} + \left(\frac{(2n-1)\pi}{2S_{Fe(\gamma)}}\right)^2}\right)^{-1} \times$$
$$\times \frac{2}{S_{Fe(\gamma)}} \int_0^{S_{Fe(\gamma)}} f_{Fe(\gamma)}(x) \cos\frac{(2n-1)\pi x}{2S_{Fe(\gamma)}} dx \tag{51}$$

$n = 1, 2, ...$

The obtained solution can easily be proved, Eq. (35) and Eq. (42), fulfils the conditions applied to the description:

$$\left.\frac{\partial \delta C(x,z)}{\partial x}\right|_{x=0} = \left.\frac{\partial \delta C(x,z)}{\partial x}\right|_{x=2S_{Fe(\gamma)}} = 0 \tag{52}$$

$$\left.\frac{\partial \delta C(x,z)}{\partial z}\right|_{z=0} = f_{Fe(\gamma)}(x) = f_{Fe(\gamma)}(-x) =$$
$$= -f_{Fe(\gamma)}(x + 2S_{Fe(\gamma)}) = -\left.\frac{\partial \delta C(-x + 2S_{Fe(\gamma)}, z)}{\partial z}\right|_{z=0} \tag{53}$$

according to the assumptions:

$$f_{Fe(\gamma)}(-x) = f_{Fe(\gamma)}(x),$$
$$f_{Fe(\gamma)}(x + 2S_{Fe(\gamma)}) = -f_{Fe(\gamma)}(x) \tag{54}$$

B) By analogy, for the Fe_3C – faceted eutectic phase:

$$x \in \left[S_{Fe(\gamma)}, S_{Fe(\gamma)} + S_{Fe_3C}\right], \quad z \geq 0$$

$$\delta C(x,z) =$$
$$= \sum_{n=1}^{\infty} \left[B_{2n-1} \cos\left(\frac{(2n-1)\pi\left(x - S_{Fe(\gamma)} + S_{Fe_3C}\right)}{2S_{Fe_3C}}\right) \cdot \exp\left[\left(-\frac{v}{2D} - \sqrt{\frac{v^2}{4D^2} + \left(\frac{(2n-1)\pi}{2S_{Fe_3C}}\right)^2}\right) z\right] \right] \tag{55}$$

$$B_{2n-1} = \left(-\frac{v}{2D} - \sqrt{\frac{v^2}{4D^2} + \left(\frac{(2n+1)\pi}{2S_{Fe_3C}}\right)^2}\right)^{-1} \frac{2}{S_{Fe_3C}} \times$$
$$\times \int_{S_{Fe(\gamma)} - S_{Fe_3C}}^{S_{Fe(\gamma)}} f_{Fe_3C}(x) \cos\frac{(2n+1)\pi\left(x - S_{Fe(\gamma)} + S_{Fe_3C}\right)}{2S_{Fe_3C}} dx \tag{56}$$

For solidification from [7,8,12]:

$$\delta C(x,z) =$$
$$= \sum_{n=1}^{\infty} B_{2n-1} \cos\left(\frac{(2n-1)\pi\left(x - S_{Fe(\gamma)} + S_{Fe_3C}\right)}{2S_{Fe_3C}}\right) \times$$
$$\times \exp\left(-\frac{(2n-1)\pi}{2S_{Fe_3C}} z\right) \tag{55*}$$

$$B_{2n-1} = -\frac{4}{(2n-1)\pi} \int_{S_{Fe(\gamma)} - S_{Fe_3C}}^{S_{Fe(\gamma)}} f_{Fe_3C}(x) \times$$
$$\times \cos\frac{(2n-1)\pi\left(x - S_{Fe(\gamma)} + S_{Fe_3C}\right)}{2S_{Fe_3C}} dx \tag{56*}$$

with:

$$\left.\frac{\partial \delta C(x,z)}{\partial z}\right|_{z=0} = f_{Fe_3C}(x), \quad x \in \left[0, S_{Fe_3C}\right] \tag{57}$$

The relationship between A_{2n-1} and B_{2n-1} [17] is:

$$B_{2n-1} = A_{2n-1}\left(\frac{S_{Fe(\gamma)}}{S_{Fe_3C}}\right)^2, \quad n = 1, 2... \tag{58}$$

The solution obtained should be verified using the so-called local mass balance calculation:

$$\int_0^{S_{Fe(\gamma)}} \delta C(x, 0) dx + \int_{S_{Fe(\gamma)}}^{S_{Fe(\gamma)} + S_{Fe_3C}} \delta C(x, d) dx = 0 \tag{59}$$

Local mass balance, Eq. (59), is fulfilled provided that d_{Fe_3C} is taken into account – the protrusion of the leading eutectic phase Fe_3C over the wetting eutectic phase $Fe(\gamma)$. This

theoretical conclusion is justified, as the phase protrusion has been observed experimentally.

Furthermore, according to the assumption of coupled eutectic growth, $\Delta T_{Fe_3C} \neq \Delta T_{Fe(\gamma)}$, Eq. (22), the protrusion is to be expected. Eq. (59) results in:

$$\sum_{n=1}^{\infty} A_{2n-1} \frac{2S_{Fe(\gamma)}(-1)^{n-1}}{(2n-1)\pi} - \sum_{n=1}^{\infty} B_{2n-1} \frac{2S_{Fe_3C}(-1)^{n-1}}{(2n-1)\pi} \times$$

$$\times \exp\left(-\frac{vS_{Fe_3C} + \sqrt{v^2 S_{Fe_3C}^2 + (2n-1)^2 D^2 \pi^2}}{2DS_{Fe_3C}}d\right) = 0 \quad (60)$$

For solidification from [7,8,12]:

$$\sum_{n=1}^{\infty} A_{2n-1} \frac{(-1)^{n-1}}{(2n-1)}\left(1 - \frac{S_{Fe(\gamma)}}{S_{Fe_3C}}\exp\left(-\frac{(2n-1)\pi}{2S_{Fe_3C}}d\right)\right) = 0 \quad (61)$$

Figure 2 shows interlamellar (interphase) spacing λ as a geometric parameter as follows:

$$\lambda = 2\left(S_{Fe_3C} + S_{Fe(\gamma)}\right) \quad (62)$$

thus:

$$S_{Fe(\gamma)} = \frac{\lambda}{2} - S_{Fe_3C} \quad (63)$$

For the studied directionally solidified Fe-4.25%C eutectic alloy, the relationship between interphase (interlamellar) spacing λ and growth rate v, is given by the formula from [12]:

$$\lambda = -0.0405v^{-0.5} + 11.499 \quad (64)$$

thus:

$$S_{Fe(\gamma)} = \frac{-0.0405v^{-0.5} + 11.499}{2} - S_{Fe_3C} \quad (65)$$

Substituting Eq. (65) to formula Eq. (61):

$$\sum_{n=1}^{\infty} A_{2n-1} \frac{(-1)^{n-1}}{(2n-1)} \times$$

$$\times \left(1 - \frac{\frac{-0.0405v^{-0.5}+11.499}{2} - S_{Fe_3C}}{S_{Fe_3C}} \exp\left(-\frac{(2n-1)\pi}{2S_{Fe_3C}}d\right)\right) = 0$$

$$\sum_{n=1}^{\infty} A_{2n-1} \frac{(-1)^{n-1}}{(2n-1)} \times$$

$$\times \left(1 - \frac{\frac{1}{2}\left(-0.0405v^{-0.5}+11.499\right) - S_{Fe_3C}}{S_{Fe_3C}} \exp\left(-\frac{(2n-1)\pi}{2S_{Fe_3C}}d\right)\right) = 0 \quad (66)$$

The above equation will be met if for each n:

$$A_{2n-1} = 0; \text{ or } \frac{(-1)^{n-1}}{(2n-1)} = 0, \text{ which is only met for } n = \infty; \text{ or:}$$

$$\left(1 - \frac{\frac{1}{2}\left(-0.0405v^{-0.5}+11.499\right) - S_{Fe_3C}}{S_{Fe_3C}} \times \exp\left(-\frac{(2n-1)\pi}{2S_{Fe_3C}}d\right)\right) = 0 \quad (67)$$

after rearrangements:

$$\frac{\frac{1}{2}\left(-0.0405v^{-0.5}+11.499\right) - S_{Fe_3C}}{S_{Fe_3C}} \times \exp\left(-\frac{(2n-1)\pi}{2S_{Fe_3C}}d\right) = 1 \quad (68)$$

which reduces to:

$$\frac{-0.02025v^{-0.5} + 5.7495 - S_{Fe_3C}}{S_{Fe_3C}} \times \exp\left(-\frac{(2n-1)\pi}{2S_{Fe_3C}}d\right) = 1 \quad (69)$$

logarithmized:

$$\ln\left(\frac{-0.02025v^{-0.5} + 5.7495 - S_{Fe_3C}}{S_{Fe_3C}} \times \exp\left(-\frac{(2n-1)\pi}{2S_{Fe_3C}}d\right)\right) = \ln(1) \quad (70)$$

the sum of logarithms on both sides was obtained:

$$\ln\left(\frac{-0.02025v^{-0.5} + 5.7495 - S_{Fe_3C}}{S_{Fe_3C}}\right) + \ln\left(\exp\left(-\frac{(2n-1)\pi}{2S_{Fe_3C}}d\right)\right) = 0 \quad (71)$$

which reduces to:

$$\ln\left(\frac{-0.02025v^{-0.5} + 5,7495 - S_{Fe_3C}}{S_{Fe_3C}}\right) + \frac{(2n-1)\pi}{2S_{Fe_3C}}d = 0 \quad (72)$$

rearranged to:

$$\frac{(2n-1)\pi}{2S_{Fe_3C}}d = \ln\left(\frac{-0.02025v^{-0.5} + 5.7495 - S_{Fe_3C}}{S_{Fe_3C}}\right) \quad (73)$$

1186

eventually resulting in:

$$d = \frac{2 S_{Fe_3C} \ln\left(\dfrac{-0.02025 v^{-0.5} + 5.7495 - S_{Fe_3C}}{S_{Fe_3C}}\right)}{(2n-1)\pi} \quad (74)$$

Eq. (74) defines protrusion d of leading cementite phase obtained according to Wołczyński model.

5. Concluding remarks

After rapid quenching of directionally solidified of Fe-4.25% C eutectic alloy [7,8,12], protrusion and delay of eutectic phases were observed**. Protrusion and delay of these phases ensure a mass balance at the solid/liquid interface of the growing eutectic alloy Fe-4.25% C.

Using current mathematical analysis, it is possible to calculate the protrusion of leading cementite phase and delay of wetting austenite phase.

The mass diffusion equation was used in both models. In each model, different parameters describing the solidifying alloy were used. Different boundary conditions and mass balance conditions at the solid/liquid border were also determined. This allowed to present the concentration field in the liquid phase ahead of the solid/liquid interface.

The analysis, according to Guzik model, showed that equation (29) presents the relationship between protrusion d_{Fe_3C} of leading phase and eutectic growth rate v. Another relationship of these parameters shows the equation (74) according to Wołczyński model.

In the Guzik model, the total protrusion d is the sum of the protrusion d_{Fe_3C} of leading cementite phase Eq. (26) and the delay $d_{Fe(\gamma)}$ of wetting austenite phase Eq. (27). In the Wołczyński model, the calculated protrusion d, Eq. (74), is a protrusion of leading phase (cementite) over the wetting phase (austenite).

Equation (29) from the Guzik model shows that the function describing the relationship between protrusion of cementite d_{Fe_3C} and growth rate v is polynomial. Variable v (growth rate), in this polynomial function, is in a base of multiple exponential expressions with different exponents.

In the Eq. (74) obtained using the Wołczyński model, the mathematical relationship between protrusion d and growth rate v is logarithmic.

The protrusion of cementite parameters obtained in the calculations of these two models cannot be compared. The nature of protrusion for equation (29) and (74) is different. The behaviour of the protrusion of leading parameter is different in both models.

REFERENCES

[1] E. Cadirli, H. Kaya, M. Gunduz, Materials Research Bulletin **38**, 1457-1476 (2003).

[2] G.J. Davies, Solidification and casting, Wiley (1973).

[3] V.L. Davies, Journal of the Institute of Metals **93**, 10-14 (1964-65).

[4] M. Hillert, V.V. Subba Rao, Iron and Steel Intitute Publication **110**, 204-212 (1968).

[5] D.M. Stefanescu, Eutectic solidification, Science and Engineering of Casting Solidification, Springer 207 (2015).

[6] E. Fraś, Krystalizacja metali, Wydawnictwo Naukowo Techniczne, Warszawa (2003).

[7] M. Trepczyńska-Łent, Archives of Foundry Engineering **13** (3), 101-106 (2013).

[8] M. Trepczyńska-Łent, Archives of Metallurgy and Materials **58** (3), 987-991. (2013). DOI: https://doi.org/10.2478/amm-2013-0116

[9] M. Trepczyńska-Łent, Archives of Foundry Engineering **16** (4), 169-174 (2016). DOI: https://doi.org/10.1515/afe-2016-0104

[10] M. Trepczyńska-Łent, Archives of Metallurgy and Materials **62** (1), 365-368 (2017). DOI: https://doi.org/10.1515/amm-2017-0056

[11] M. Trepczyńska-Łent, Crystal Research and Technology **52** (7), 1600359 (2017). DOI: https://doi.org/10.1002/crat.201600359

[12] M. Trepczyńska-Łent, Archives of Foundry Engineering **19** (4), 113-116 (2019).

[13] E. Guzik, A model of irregular eutectic growth taking as an example the graphite eutectic in Fe-C alloys. Dissertations Monographies 15, AGH Kraków (1994).

[14] P. Magnin, W. Kurz, Acta Metall. **35**, 1119 (1987).

[15] J.D Hunt., K.A Jackson, Trans Metall. Soc. AIME **236**, 843-852 (1966).

[16] K.A. Jackson, J.D. Hunt, Transactions of the Metallurgical Society of AIME **236**, 1129-1142 (1966).

[17] W Wołczyński, Defect and Diffusion Forum **272**, 123-138 (2007).

[18] W. Wołczyński, Archives of Metallurgy and Materials **63** (1), 65-72 (2018).

[19] G.A Chadwick, Eutectic Alloy Solidification, Chapter 2 in: Progress in Materials Science. Pergamon Press, Headington Hill Hall, Oxford (1964).

[20] W. Wołczyński, Crystal Research and Technology **25** (1), 1303-1309 (1990).

[21] W. Wołczyński, Archives of Metallurgy and Materials **65** (2), 653-666 (2020). DOI: https://doi.org/10.24425/amm.2020.132804